Conversion of 7-ketocholesterol to oxysterol metabolites by recombinant CYP27A1 and retinal pigment epithelial cells[S]

Gun-Young Heo,* Ilya Bederman,[†] Natalia Mast,* Wei-Li Liao,[1,§] Illarion V. Turko,[§,**] and Irina A. Pikuleva[2,*]

Departments of Ophthalmology and Visual Sciences,* and Pediatrics,[†] Case Western Reserve University, Cleveland, OH; Institute for Bioscience and Biotechnology Research,[§] Rockville, MD; and Division Analytical Chemistry,** National Institute of Standards and Technology, Gaithersburg, MD

Abstract Of the different oxygenated cholesterol metabolites, 7-ketocholesterol (7KCh) is considered a noxious oxysterol implicated in the development of certain pathologies, including those found in the eye. Here we elucidated whether sterol 27-hydroxylase cytochrome P450 27A1 (CYP27A1) is involved in elimination of 7KCh from the posterior part of the eye: the neural retina and underlying retinal pigment epithelium (RPE). We first established that the affinities of purified recombinant CYP27A1 for 7KCh and its endogenous substrate cholesterol are similar, yet 7KCh is metabolized at a 4-fold higher rate than cholesterol in the reconstituted system in vitro. Lipid extracts from bovine neural retina and RPE were then analyzed by isotope dilution GC-MS for the presence of the 7KCh-derived oxysterols. Two metabolites, 3β,27-dihydroxy-5-cholesten-7-one (7KCh-27OH) and 3β-hydroxy-5-cholesten-7-one-26-oic acid (7KCh-27COOH), were detected in the RPE but not in the neural retina. 7KCh-27OH was also formed when RPE homogenates were supplemented with NADPH and the mitochondrial redox system. Quantifications in human RPE showed that CYP27A1 is indeed expressed in the RPE at 2-4-fold higher levels than in the neural retina.▮▮ The data obtained represent evidence for the role of CYP27A1 in retinal metabolism of 7KCh and suggest that, in addition to cholesterol removal, the functions of this enzyme could also include elimination of toxic endogenous compounds.—Heo, G-Y., I. Bederman, N. Mast, W-L. Liao, I. V. Turko, and I. A. Pikuleva. **Conversion of 7-ketocholesterol to oxysterol metabolites by recombinant CYP27A1 and retinal pigment epithelial cells.** *J. Lipid Res.* **2011.** 52: 1117–1127.

Supplementary key words 3β,27-dihydroxy-5-cholesten-7-one • 3β-hydroxy-5-cholesten-7-one-26-oic acid• isotope dilution gas chromatography-mass spectrometry • age-related macular degeneration • cytochrome P450 27A1

7-Ketocholesterol (3β-hydroxy-5-cholesten-7-one or 7KCh), a product of cholesterol auto-oxidation and an oxysterol, attracts constant attention because of its deleterious pro-inflammatory and pro-apoptotic effects in vitro (reviewed in Refs. 1–4). However, it still remains to be proven whether these in vitro properties are of physiological relevance. 7KCh is the most abundant oxysterol of nonenzymatic origin in atherosclerotic plaques, indicating that it may play a role in the initiation and/or development of atherosclerosis (2, 5). In the eye, 7KCh was found in human cataracts, but it was not detected in clear lenses (6). Experimental data suggest that 7KCh disrupts the highly regulated differentiation program of the lens epithelial cells, thus compromising lens growth and transparency (7). Studies on monkeys demonstrate that 7KCh is also present at very low levels in the neural retina and at 3-5-times higher levels in the retinal pigment epithelium (RPE)-choriocapillaris region beneath the neural retina (8). Similarly, low levels of 7KCh were found in the retina of untreated rats, but exposure to intense, constant light increased the levels of 7KCh ∼6-fold (9). In light-exposed

---

rats, 7KCh was observed in both the RPE-choriocapillaris region and neural retina, and in the latter, 7KCh was immunolocalized to the regions with high mitochondrial content, the ganglion cell layer and photoreceptor inner segments (9). 7KCh is studied in the retina because of the possible connection to age-related macular degeneration (4), a major cause of blindness in the elderly in industrialized countries (10). Loss of vision in age-related macular degeneration is caused by degeneration of the neural retina and RPE in the macula (11), a region near the center of the retina.

7KCh is putatively a toxic compound, yet the mechanisms whereby it is formed and eliminated in vivo are not fully understood. Evidence was obtained indicating that iron is likely involved in generation of 7KCh in the neural retina (9). The source of iron was not determined, but ferritin and/or cytochrome c are suspected (4). The routes of 7KCh elimination from the retina are also under investigation. Four pathways are considered: *i*) enzymatic oxidation by cholesterol 25-hydroxylase and cytochrome P450 enzymes 27A1 and 46A1 (CYP27A1 and CYP46A1); *ii*) reduction by 11β-hydroxysteroid dehydrogenase type 1; *iii*) efflux involving transporters such as ABCA1 and ABCG5; and *iv*) sulfonation by sulfotransferases (reviewed in Ref. 4). Of these four possible pathways, we favor enzymatic oxidation of 7KCh by CYP27A1, a ubiquitous sterol 27-hydroxylase with relatively broad substrate specificity and multiple physiological roles. Indeed, CYP27A1 is involved in cholesterol elimination from extrahepatic tissues, metabolizes bile acid intermediates in the liver, and activates vitamin D_3 in the kidney (12–14). CYP27A1 is also a mitochondrial protein whose immunolocalization in the retina overlaps with that of 7KCh: photoreceptor inner segments, ganglion cell layer, and RPE (15). Furthermore, 7KCh was found to be 27-hydroxylated in human macrophages and HepG2 cells (16, 17); it was suggested to be the substrate for CYP27A1 based on the site of hydroxylation, reduction of its metabolism by the cells treated with several CYP27A1 inhibitors, and absence of 27-hydroxylated 7KCh metabolite in the medium when CYP27A1-deficient human macrophages were incubated with exogenous radioactive 7KCh (16). These studies, however, did not assess whether enzymes other than CYP27A1 were also inhibited and whether CYP27A1 deficiency affected the uptake of exogenous radioactive 7KCh by the cultured cells.

CYP27A1 is a strong candidate for being the major enzyme eliminating 7KCh in the retina. Yet, in previous studies by others, hydroxylated products of 7KCh were not detected either in monkey retina or photodamaged rat retina when retinal lipid extracts were analyzed by high performance liquid chromatography (HPLC) coupled to mass spectrometry (MS) based on atmospheric pressure chemical ionization (8, 9). Therefore, in the present work, we investigated retinal metabolism of 7KCh by a highly sensitive analytical tool, isotope dilution gas chromatography-mass spectrometry (GC-MS) with selected ion monitoring (SIM) following in vitro studies evaluating 7KCh as a substrate for purified recombinant CYP27A1. We show here that 7KCh was efficiently hydroxylated several times

by CYP27A1 in the reconstituted system in vitro and present evidence that this P450 also oxidized 7KCh in vivo in bovine RPE. Our results suggest that cytochrome P450-mediated metabolism could be at least one of the mechanisms whereby RPE removes toxic 7KCh, thus expanding our understanding of the retinal significance of CYP27A1.

MATERIALS AND METHODS

Materials

Cholesterol and 7KCh were purchased from Steraloids, Inc. (Newport, RI); [25,26,26,26,27,27,27-$^2H_7$]cholesterol (cholesterol-D_7) and [26,26,26,27,27-$^2H_5$]27-hydroxycholesterol (27OH-D_5) were from Medical Isotopes (Pelham, NH); [25,26,26,26,27,27,27-$^2H_7$]7KCh (7KCh-D_7) was from CDN Isotopes (Quebec, Canada); [^3H]7KCh and [^3H]cholesterol were from American Radiolabeled Chemicals, Inc. (St. Louis, MO); 27OH, 7KCh-27OH and 7KCh-27COOH were from Avanti (Alabaster, AL). Human recombinant CYP27A1, mitochondrial redox partners adrenodoxin (Adx) and adrenodoxin reductase (Adr), and microsomal P450 oxidoreductase were expressed and purified as described (18–21). Bovine eyes were obtained from a local slaughterhouse 3–5 h after animals were sacrificed. The anterior segment was removed, and the vitreous humor was poured out to expose the retina. The neural retina was carefully separated from the RPE, placed in a tube, and washed one time (by centrifugation at 2,000 *g*) with PBS. The remaining eye cup was incubated on ice with 5 ml of PBS containing 1 mM EDTA to chelate Ca^{2+} and facilitate dissociation of the RPE from the basement membrane (22). In 30 min, the RPE was gently brushed off, aspirated, and subjected to repeated washes by differential centrifugation (23) until the supernatant was clear and colorless and the pelleted RPE cells were essentially free of the contaminating nonmelanotic cells, erythrocytes, and rod outer segments as assessed by brightfield microscopy. Fluorescent microscopy (excitation at 488 and emission at 515 nm) did not detect autofluorescent rod outer segments, erythrocytes, or macrophages, thus confirming the analysis done by light microscopy. The isolated RPE was either used immediately or flash-frozen in liquid nitrogen and stored at −80°C. Cadaveric human eyes were processed previously (24). The RPE was gently scraped under the dissecting microscope with a crescent knife, aspirated with a glass microcapillary tube, and frozen. Assessment of the purity of these preparations by brightfield and fluorescent microscopies did not reveal significant contaminations: only few nonmelanotic nonautofluorescent cells of undetermined origin were present. Human tissue use conformed to the Declaration of Helsinki and institutional review at Case Western Reserve University. Eye specimens were obtained from de-identified donors following informed consent of their families.

Isolation of mitochondrial phospholipids (PL) from bovine neural retina and RPE and preparation of PL vesicles for the enzyme assay

Each tissue (∼5 g) was homogenized with Teflon grinder in 10 ml of 50 mM Tris-HCl (pH 7.4), containing 250 mM sucrose, 5 mM $MgCl_2$, 1 mM phenylmethylsulfonyl fluoride, 1 mM dithiotreitol, 100 μg/ml of butylated hydroxytoluene (BHT), and a cocktail of protease inhibitors (Roche Complete EDTA-free, 1 tablet/50 ml buffer). Tissue homogenates were subjected to centrifugation at 1,000 *g* for 20 min to remove unbroken cell, nuclei, and cell debris followed by centrifugation of the resultant supernatant at 9,000 *g* for 20 min to pellet the mitochondria. Mitochondria were resuspended in 3 ml of the homogenization buffer

(~5 mg protein/ml) with the Tris-HCl concentration reduced to 10 mM, and then mixed with 6 ml of the Folch reagent (chloroform-methanol, 2:1, V/V) (25) by vigorous vortexing for 30 s. Phase separation was facilitated by centrifugation at 2,000 *g* for 10 min; the lower organic phase was removed, placed in a glass tube, and dried under the nitrogen gas. Subsequent separation of nonphosphorous lipids and PLs was as described (26). Briefly, lipid extract was dissolved in 100 μl of chloroform and applied on a dry 690 mg Sep-Pak Silica Cartridge (Waters Corporation, Milford, MA). The cartridge was first washed with 20 ml of chloroform to elute nonphosphorous lipids and then with 30 ml of methanol to elute PLs. Both nonphosphorous lipids and PLs were dried under the nitrogen gas and redissolved in 2 ml of chloroform. Absence of cholesterol and other nonphosphorous lipids in the PL fraction was confirmed by thin layer chromatography (TLC) on plates with silica gel using hexane/diethyl ether/methanol/acetic acid (90/20/5/2, V/V/V/V) as resolving mobile phase; bands were detected by iodine. The PL concentration was measured using ammonium ferrothiocyanate as described (27). The calibration curve was generated using known amounts of 1-palmitoyl-2-oleoyl-sn-glycero-3-[phosphor-rac-1(1-glycerol)]. Stock solution of PL vesicles for reconstitution with CYP27A1 was prepared by evaporating 1 mg of PL solution in chloroform in a glass tube, then adding 1 ml of 40 mM potassium phosphate buffer (KPi), pH7.2, containing 1 mM EDTA, vortexing, and placing the glass tube in an ice-water bath that was sonicated for 15 min with a Digital Sonifier (Branson, Danbury, CT) at a 50% amplitude.

Enzyme assays with purified recombinant human CYP27A1

In studies assessing the ability to hydroxylate 7KCh, 0.02 μM or 0.2 μM CYP27A1 was reconstituted with 2 μM 7KCh, 100,000 cpm of [^{3}H]7KCh, Adx and Adr used at 30- and 4-fold molar excesses over CYP27A1, respectively, and NADPH-regenerating system (1 mM NADPH, 1 U of isocitrate dehydrogenase, and 5 mM trisodium isocitrate). Enzymatic reactions proceeded at 37°C in 1 ml of 40 mM KP$_i$ buffer, pH 7.4, containing 1 mM EDTA, and were terminated by addition of 5 ml of methanol:chloroform (2:1, V/V). The two phases were separated by a 10 min-centrifugation at 2,000 *g*; the lower phase was isolated and dried under nitrogen (25). The dried extract was then dissolved in 100 μl of acetonitrile:methanol:H$_2$O (50:20:30, V/V) and subjected to HPLC using a Shimadzu HPLC system (Tokyo, Japan) with a Nova-Pak C$_{18}$ column (3.9 × 150 mm, Waters, Millford, MA) connected to a β-RAM radioactivity detector (INUS Systems Inc., Tampa, FL). The flow rate (1 ml/min) was kept at 100% solvent A (acetonitrile:methanol:water, 50:20:30, V/V) for 5 min, then a linear gradient between solvent A and solvent B (100% methanol) over 15 min was used, after which the flow was kept at 100% solvent B for another 5 min. Peak areas corresponding to 7KCh and its metabolites were integrated and used to calculate the substrate metabolism.

To identify metabolites of 7KCh, a separate enzyme assay was carried out, in which only unlabeled 7KCh was used. The concentrations of CYP27A1 and 7KCh were 0.2 μM and 2 μM, respectively, and those of Adx and Adr were 6 μM and 0.8 μM, respectively; the reaction time was 5 min. The products were isolated by HPLC, followed by analysis by GC-MS.

To determine the rates of cholesterol and 7KCh hydroxylation, a third set of experiments was conducted in which 0.05 μM CYP27A1 was added to 1 ml of 40 mM KP$_i$, pH 7.4, containing 1 mM EDTA, 20 μg of PLs, 30 μM cold sterol substrate, ~1 nM [^{3}H]labeled sterol substrate (100,000 cpm), 1.5 μM Adx, and 0.2 μM Adr. The assay mixture was incubated at room temperature for 30 min and then at 37°C for additional 10 min followed by the

addition of the NADPH-regenerating system to initiate the enzyme reaction, which was carried out for 2 min.

Spectral binding assay with purified recombinant human CYP27A1

Titrations with cholesterol and 7KCh were carried out at 30°C as described (28). Sterols were added from 1 mM stock in 4.5% aqueous 2-hydroxypropyl-β-cyclodextrin to a 1-ml solution of 50 mM KP$_i$, pH 7.2, containing 0.4 μM CYP27A1, 1 mM EDTA, 0.5 M NaCl, and 10% glycerol. The K$_d$ values were calculated by nonlinear least-squares fitting using the quadratic form of the single-site binding equation (29):

$$\Delta A = 0.5\, \Delta A_{max} \left(K_d + [E] + [S] - \sqrt{(K_d + [E] + [S])^2 - 4[E][S]} \right) \ \textit{(Eq. 1)}$$

where ΔA is the spectral response at different substrate concentrations [S], ΔA$_{max}$ is the maximal amplitude of the spectral response, and [E] is the enzyme concentration.

Quantification of sterols in bovine tissues

Fresh neural retina or RPE was weighed and homogenized in 10 vol (w/v) of 40 mM KP$_i$, pH 7.2, containing 1 mM EDTA and 100 μg/ml BHT. Tissue homogenization was followed by centrifugation at 1,500 *g* for 15 min to remove cell debris. Supernatant aliquots (~15 mg of total protein per tube) were used either for lipid extraction or enzyme assays. For the former, two tubes were used, each supplemented with the same amounts of cholesterol-D$_7$ (500 nmol) and 27OH-D$_5$ (1 nmol) but different amounts of 7KCh-D$_7$ (0.2 or 0.02 nmol) for quantification of 7KCh and 7KCh-27OH, respectively. Lipids were extracted from tissue homogenates five times by vortexing with 2.5 vol of chloroform/methanol (2:1, V/V) for 1 min. The chloroform phases were combined and evaporated to dryness at room temperature under vacuum using a Savant SC2104 SpeedVac Concentrator (Thermo Scientific, Ashville, NC). Oxysterols were separated from cholesterol by solid phase extraction as described (30). Briefly, the dried lipid extract was dissolved in 10 ml of 70% ethanol and applied to a Varian C18 SPE column (1000 mg, Varian Inc., Lake Forest, CA) equilibrated with 30 ml of 70% ethanol. The flow-through fraction was collected and combined with the eluate from the subsequent column wash with 40 ml of 70% ethanol. The combined eluates represented the oxysterol fraction. The cholesterol fraction was eluted next by washing the column with 20 ml of ethanol. The oxysterol and cholesterol fractions were evaporated to dryness in a SpeedVac Concentrator and methylated with 3 ml of freshly prepared ethereal diazomethane at room temperature for 30 min. After methylation, the fractions were dried under nitrogen, derivatized with 60 μl of bis-(trimethylsilyl)trifluoroacetamide/trimethylchlorosilane (TMS) at 60°C for 1 h, and subjected to GC-MS.

Saponification was performed on a dried lipid extract as described (31). Briefly, 2 ml of 20% KOH in methanol was added and vortexed to dissolve lipids. Then 2 ml of diethyl ether was added, followed by vortexing and flushing the solution with nitrogen to remove air. The solution was vigorously shaken on ice for 3 h in a capped glass tube, then the reaction was stopped by 20% acetic acid (2 ml). Hexane (2.5 ml) was added, and the upper phase was isolated and dried. The dried extract was dissolved in 10 ml of 70% ethanol and used for separation on a Varian C18 SPE column as described above.

GC-MS analysis

The derivatized samples were analyzed using an Agilent 5973N-MSD mass spectrometer equipped with an Agilent 6890 gas chromatograph. A DB-35ms (Agilent Technologies, Santa Clara, CA)

capillary column (30 m × 0.25 mm × 0.25 mm) was used for all analyses. The mass spectrometer was operated in the electron impact (EI) ionization mode. Gas chromatographic conditions were as follows: 2 µl sample was injected in splitless mode (inlet was kept at 270°C with the helium flow at 1.0 ml/min) at the initial 150°C. The oven was first kept at 150°C for 2 min, ramped at 10°C/min to 310°C, and held for 20 min isothermally. The ion source filament was operated at 70 eV. The mass detector was set at 310°C. We utilized both scan (total ion monitoring, m/z range of 100–700 Da) and SIM modes and the optimal dwell time (10 msec per ion). The following ions (m/z) were monitored in the SIM mode: 368 (cholesterol); 375 (cholesterol-D_7); 417 (27OH), 422 (27OH-D_5), and 472 (7KCh); 479 (7KCh-D_7); 455, 470, 545, and 560 (7KCh-27OH); and 411, 426, 501, and 516 (7KCh-27COOH). For quantification, calibration curves were generated using a fixed concentration of the internal standard, deuterated sterol analog, and varying concentrations of the corresponding unlabeled sterol.

Incubations with RPE homogenates

RPE homogenates (∼15 mg of total protein) were incubated either with 10 mM NADPH or with 10 mM NADPH plus 5 µM Adr and 15 µM Adx or with 10 mM NADPH plus 5 µM P450 oxidoreductase. Incubations were carried out for 60 min at 37°C with constant shaking. Extraction of lipids and GC-MS analysis were as described above.

RESULTS

Enzyme assays with purified recombinant human CYP27A1 and identification of 7KCh metabolites

As it had not previously been shown that purified CYP27A1 metabolizes 7KCh, two enzyme concentrations (0.02 µM and 0.2 µM) and different reaction times (up to 2 h) were tested in the in vitro reconstituted system, and then the product formation was assessed by HPLC. At 0.02 µM CYP27A1 and 5 min reaction time, only one product peak, putatively 7KCh-27OH, was seen during HPLC separation (**Fig. 1A**). Yet two product peaks were observed when the enzyme reaction proceeded for 2 h (Fig. 1B). The retention time of the second product peak was earlier than that of the putative 7KCh-27OH, indicating that it is the more polar metabolite. Consequently, by analogy with our previous studies investigating cholesterol as a substrate for CYP27A1 (32), we hypothesized that the second product was 7KCh-27COOH. The kinetics of the formation of the putative 7KCh-27OH and 7KCh-27COOH in the enzyme assay were different (Fig. 1C, D). At low CYP27A1 concentration (0.02 µM), the 7KCh-27OH content increased up to 30 min of reaction time but then started to decline. In contrast, the amount of 7KCh-27COOH was constantly increasing and reached the levels of 7KCh-27OH after 120 min of enzymatic reactions (Fig. 1C). At 10-fold higher CYP27A1 concentration (0.2 µM), 7KCh-27COOH became a predominant metabolite after only 15 min of the enzymatic reaction. After 60 min, almost all 7KCh was converted to 7KCh-27COOH (Fig. 1D). Thus, CYP27A1 can metabolize 7KCh in vitro and yield different products depending on the conditions of the enzyme assay: higher enzyme concentration and longer reaction time lead to the formation of the more polar metabolite.

This result is consistent with previous studies by us and others showing multiple oxidations of cholesterol and 5β-cholestane-3α,7α,12α-triol by CYP27A1 to yield C27 alcohol, C27 aldehyde, and C27 acid and dependence of the product profile on the enzyme concentration and reaction time (32, 33).

To confirm that 7KCh in the enzyme assay was oxidized by CYP27A1 at C27, we used GC-MS analyses. An equimolar mixture of authentic 7KCh, 7KCh-27OH, 7KCh-27COOH as well as cholesterol, 27OH, and 5-cholestenoic acid (27-COOH) was prepared. The sterols were subjected to methylation and trimethylsilylation, and column and chromatography conditions were identified that enabled good separation of all six sterols and high sensitivity of detection (supplemental Fig. IA). The limit of detection of 7KCh-27OH in this study was ∼1 pmol/injection in SIM mode (supplemental Fig. IA, inset), which is higher than 15 pmol of 7KCh-27OH/injection, reported previously (16).

Following optimization of the conditions of GC-MS, CYP27A1 was again incubated with 7KCh under conditions that produced comparable amounts of the two metabolites (0.2 µM CYP27A1, 5 min reaction time, Fig. 1D). The metabolites were isolated by HPLC and analyzed individually by GC-MS after methylation and trimethylsilylation. The HPLC peak putatively corresponding to 7KCh-27OH (retention time 13 min, Fig. 1A, B) eluted as one peak during GC (**Fig. 2A**) at the retention time of the authentic 7KCh-27OH (supplemental Fig. I) with a fragmentation pattern very similar to that of the authentic standard (supplemental Fig. IB): a prominent molecular ion at m/z 560 (M) and fragment ions at 545 (M-15), 470 (M-90), and 455 (M-90-15) (Fig. 2C). The HPLC peak putatively corresponding to 7KCh-27COOH (retention time 8.5 min, Fig. 1A, B) eluted as three peaks during GC, one major and two smaller peaks (Fig. 2B) with the retention time of the major peak (34.8 min) corresponding to that of the authentic 7KCh-27COOH (supplemental Fig. I) and mass spectrum similar to that of authentic 7KCh-27COOH (supplemental Fig. IB): a prominent molecular ion at m/z 516 and fragment ions at 501 (M-15), 426 (M-90), and 411 (M-90-15) (Fig. 2D). We did not identify the smaller peaks in Fig. 2B because they were nonsterol compounds. Thus, similar to endogenous substrates cholesterol and 5β-cholestane-3α,7α,12α-triol, 7KCh could be oxidized CYP27A1 multiple times, yielding hydroxylated and carboxylated products. Identification of 7KCh-27COOH and its MS characterization enabled future search of this metabolite in biological samples.

Comparison of 7KCh and cholesterol as substrates for CYP27A1

Next we determined affinities of purified recombinant CYP27A1 for 7KCh and cholesterol (**Table 1**). The K_d values were found to be similar (0.07 µM for 7KCh and 0.14 µM for cholesterol), indicating that in the inner mitochondrial membrane where CYP27A1 resides and cholesterol content is low (34), 7KCh could compete with cholesterol for the CYP27A1 active site. Then we determined the
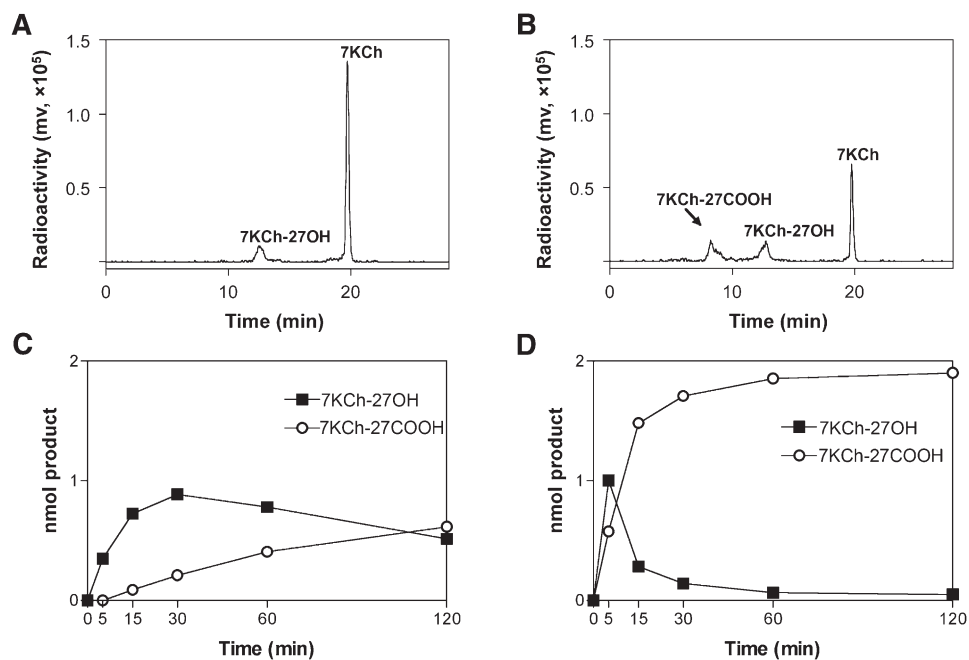
Fig. 1. Product formation in the incubations of CYP27A1 with 7KCh. A, B: Chromatograms of HPLC separation of the products formed after 5 min and 120 min of enzymatic reaction, respectively, when the concentration of CYP27A1 in the enzyme assay was 0.02 μM. C, D: Kinetics of the product formation with 0.02 and 0.2 μM CYP27A1, respectively. In all assays, the concentration of 7KCh was 2 μM, and the reaction volume was 1 ml. The results represent the average of triplicate measurements ± SD. The error bars are not seen because they are smaller than the symbol size.

rate of 7KCh and cholesterol hydroxylation in the in vitro enzyme assay. Mitochondrial PLs were isolated from bovine neural retina and RPE and used for reconstitution with CYP27A1 in the presence of saturating substrate and redox partner concentrations. The conditions of the assay were optimized for the formation of only one metabolite, 27-alcohol, with the product formation linear with time and enzyme concentration. Under these steady-state conditions, the rate of 7KCh hydroxylation was about 4-fold higher than that of cholesterol in both retinal and RPE
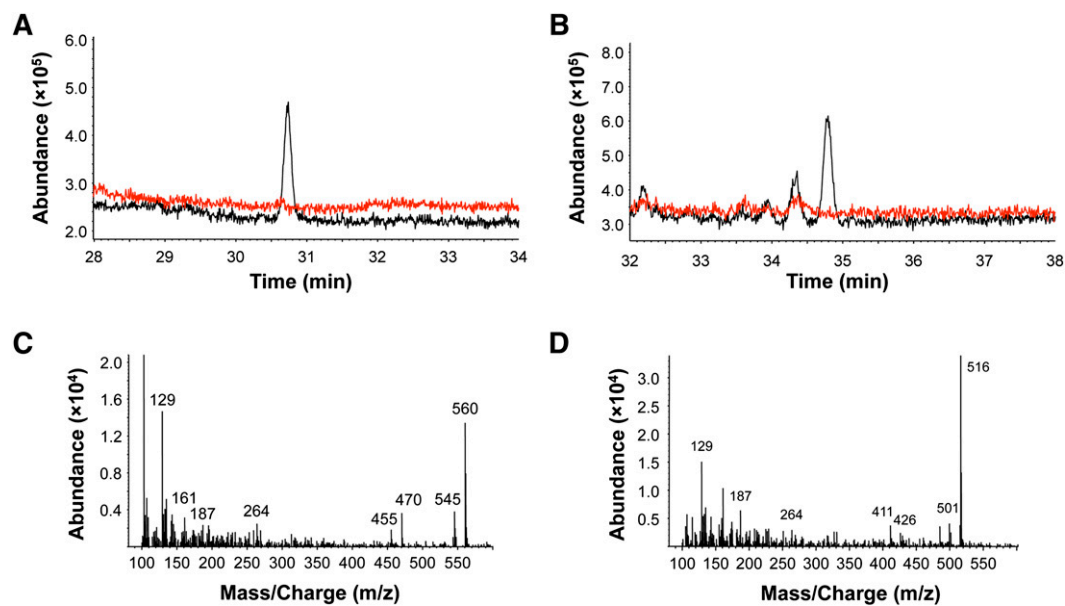
Fig. 2. Total ion chromatograms (A and B, black traces) and mass spectra (C and D) of the 7KCh metabolites (after methylation and trimethylsilylation) formed in the enzyme assay (5 min at 37°C) with 0.2 nmol of purified recombinant CYP27A1 and 2 nmol of 7KCh. The products were isolated by HPLC, and each was analyzed individually by GC-MS. Red traces show the negative control, in which CYP27A1 was boiled prior to initiation of the enzyme reaction.

TABLE 1. Spectral binding properties and enzymatic activity of CYP27A1 against cholesterol and 7KCh

| | $K_d{}^a$ (μM) | $\Delta A_{max}{}^b$ | Turnover Number (min^{-1})^c | |
			Retinal PL	RPE PL
Cholesterol	0.14 ± 0.03	0.05 ± 0.01	10.56 ± 0.37	9.28 ± 0.61
7KCh	0.07 ± 0.01	0.12 ± 0.01	40.40 ± 2.51	36.28 ± 1.48

[a] Calculated on the basis of the spectral binding.
[b] Maximal amplitude of the substrate-induced spectral response per nanomol of CYP27A1.
[c] Assessed by enzyme activity assay as described in Material and Methods. The results represent the average of triplicate measurements ± SD.

PLs (Table 1). Along with the binding data, this result suggested that 7KCh has a potential to be a substrate for CYP27A1 in vivo, and it justified our subsequent search of 7KCh metabolites in bovine neural retina and RPE.

Analysis of retinal and RPE extracts for the presence of 7KCh and its metabolites

Several precautions were taken to avoid artificial auto-oxidation of cholesterol to 7KCh during the workup of biological samples (35). Only tissues immediately isolated from fresh bovine eyes (3-5 h postmortem according to the slaughterhouse) were used, and BHT and EDTA were always included in the buffer for tissue homogenization. Lipid extracts were always evaporated at room temperature under vacuum, followed by the rapid separation of the oxysterol fraction from cholesterol by using solid-phase extraction. To ensure high accuracy of the measurements, the best possible internal standard, 7KCh-D$_7$, was used because its extraction and derivatization efficiency is very similar to that of endogenous 7KCh. Also, to determine interpreparation variability, pooled samples of the neural retina and RPE were prepared four times, each time from a group of animals with different demographics (age, breed, and ratio of bulls to cows), fed either grass or grain, and sacrificed at two different slaughterhouses.

The first preparation of the neural retina and RPE was analyzed for free (unconjugated) and total (conjugated) forms of sterols. The detector was programmed in a SIM mode for the ions characteristic for 7KCh, 7KCh-D$_7$, 7KCh-27OH, and 7KCh-27COOH. In the neural retina, only molecular ions for 7KCh-D$_7$ (m/z 479) and 7KCh (m/z 472) were observed (**Fig. 3A**), which eluted as two major peaks at the retention time of the authentic 7KCh-D$_7$ and 7KCh, respectively. In this preparation, the concentration of free 7KCh in the neural retina was 25 pmol/mg protein, and it remained the same after cold saponification, indicating lack of esterification. Ion peaks for free 7KCh were also present in the RPE (Fig. 3B) but at a concentration higher than that in the neural retina (41 pmol/mg), with saponification leading to further increase in the level of the sterol to 51 pmol/mg. Unlike the neural retina, the nonsaponified extract of RPE also contained four ion peaks characteristic for 7KCh-27OH (m/z 455, 470, 545, and 560) and 7KCh-27COOH (m/z 411, 426, 501, and 516), which coeluted for each metabolite at the retention times of the authentic standards (Fig. 3B). The content of 7KCh-27OH was estimated based on the calibration curve using 7KCh-D$_7$ as internal standard and found to be 1 pmol/mg protein. We did not quantify 7KCh-27COOH because of the

lack of a good internal standard. Saponification of the RPE lipid extract led to significant reduction of the 7KCh-27OH peak and the disappearance of the 7KCh-27COOH peak, indicating decomposition of these sterols even though they were hydrolyzed on ice. Hence, all subsequent studies have been carried out only on nonsaponified extracts of RPE.

Three preparations of the RPE were additionally isolated, and all three showed similar but ~5-fold lower content of 7KCh (~8 pmol/mg protein) compared with the first preparation (**Fig. 4**). Also, no ion peaks corresponding to 7KCh-27OH and 7KCh-27COOH were observed in these preparations. Therefore, we used these samples and reconstituted them with NADPH and either mitochondrial Adr and Adx, which transfer electrons from NADPH to all mitochondrial P450s including CYP27A1, or the microsomal P450 oxidoreductase, which reduces all microsomal P450s. These experiments were carried out because tissue disruption and homogenization usually leads to quick oxidation of endogenous NADPH and, consequently, terminate the P450-mediated enzymatic reactions. These reactions, however, could be reinitiated if the homogenate is supplemented with NADPH and the P450 redox partners that may be at limiting amounts in a biological sample.

Incubations with RPE homogenates

The ion peaks characteristic for 7KCh-27OH were only observed in the ion chromatograms of the extracts from the incubations with NADPH and a mitochondrial redox system (Fig. 4). The 7KCh-27OH concentration (~1 pmol/mg protein) was similar in all three preparations. No ion peaks characteristic for 7KCh-27OH were detected in the extracts from control incubations lacking NAPDH and a redox system or from incubations with NADPH and a microsomal redox partner P450 oxidoreductase (Fig. 4). Thus, the RPE can metabolize 7KCh to 7KCh-27OH, and this enzymatic reaction is specific to a mitochondrial P450. To confirm that CYP27A1 is active under the experimental conditions used, we measured its cholesterol hydroxylase activity and the levels of 27OH formed from cholesterol. The concentration of 27OH increased ~260-fold after initiation of the enzymatic reaction with NADPH and Adr and Adx (2 versus 521 pmol/mg protein), and to a much lesser extent, ~5-fold and 3-fold, respectively, in the presence of NADPH and NADPH plus the microsomal redox partner P450 oxidoreductase (Fig. 4). Thus, even when the concentration of cholesterol in the RPE homogenate was four orders of magnitude higher than that of 7KCh,
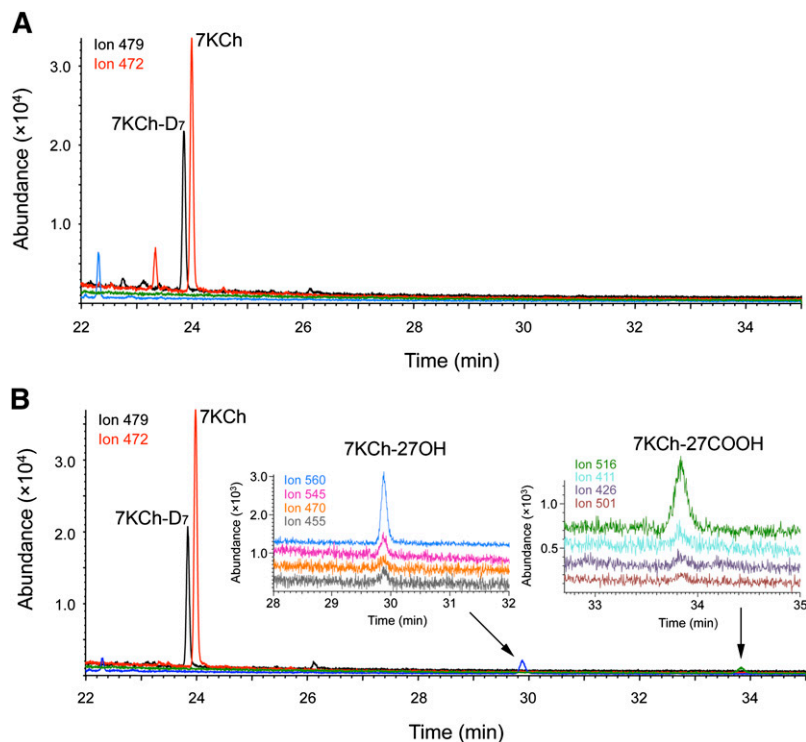
Fig. 3. SIM chromatograms of the oxysterol fractions (after methylation and trimethylsilylation) isolated from the neural retina (A) and RPE (B). Each ion trace is shown in different color: m/z 479 (black), m/z 472 (red), m/z 560 (blue), m/z 545 (magenta), m/z 470 (orange), m/z 455 (gray), m/z 516 (green), m/z 411 (cyan), m/z 426 (violet), and m/z 501 (brown). The insets show enlarged views of the chromatograms at the retention times corresponding to the elution of 7KCh-27OH and 7KCh-27COOH.

CYP27A1 was able to metabolize 7KCh, yielding 7KCh-27OH. The latter is likely because mitochondria were not significantly disrupted during homogenization and the ratio between cholesterol and 7KCh in the inner mitochondrial membrane was significantly different from that in the homogenate. Incubations with the homogenates provide additional evidence for the involvement of CYP27A1 in the metabolism of 7KCh in the RPE.
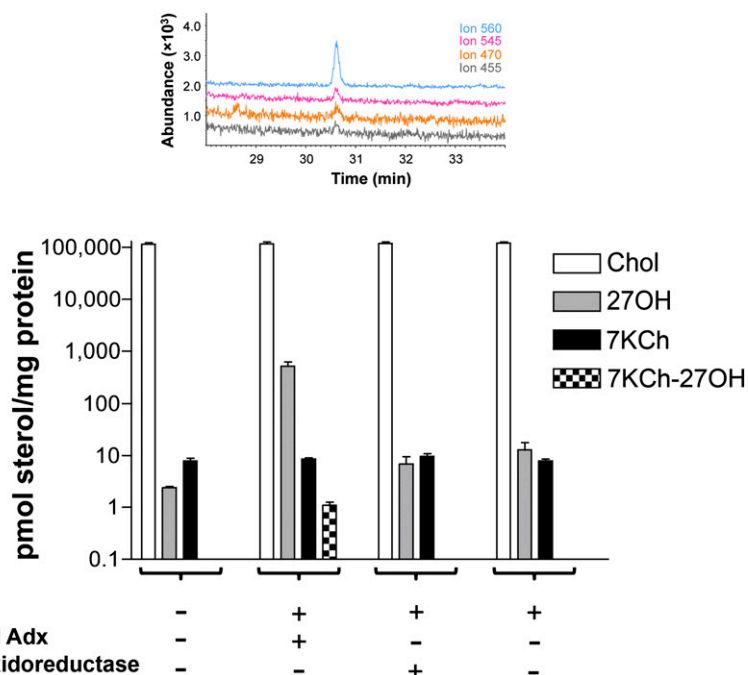

Fig. 4. Changes in sterol levels after bovine RPE homogenate was incubated with the components of the cytochrome P450 redox systems. Vertical bars (open, gray, black, and checkered) show the concentrations of cholesterol (Chol), 27OH, 7KCh, and 7KCh-27OH. The results represent the average of the triplicate measurements of each of the three RPE preparations ± SD. Where not shown, error bars are smaller than symbol size. The inset shows SIM chromatogram confirming the formation of 7KCh-27OH in the incubations with the mitochondrial redox system (5 μM adrenodoxin reductase, 15 μM adrenodoxin, and 10 mM NADPH, 1 h, 37°C). Coloring of the traces is the same as in Fig. 3.

Concentrations of CYP27A1 in the RPE

Quantifications were carried out as described (24) using multiple reaction monitoring and individual samples from four human donors. These samples were isolated during the course of our previous studies in which we measured CYP27A1 expression in the neural retina; in the present work, we determined the CYP27A1 levels in the RPE. Depending on the donor, the enzyme concentration per milligram of total protein was 2- to 4-fold higher in the RPE than in the neural retina (**Table 2**), thus confirming that CYP27A1 is indeed expressed in the RPE and providing an explanation as to why we did not detect metabolites of 7KCh in the neural retina. For each GC-MS injection, the same amount of total protein was used to extract lipids either from the neural retina or RPE. In the RPE, the levels of 7KCh metabolites were close to the limits of detection. Hence, in the neural retina, where both 7KCh and CYP27A1 are present at concentrations lower than in the RPE (per mg of protein), less 7KCh metabolites are likely generated, and these amounts may be below the limits of detection of the utilized protocol. Thus, our study does not exclude metabolism of 7KCh by CYP27A1 in the neural retina. Instead, it suggests that a higher sensitivity is required to investigate metabolism of 7KCh in this anatomical element. Note that normalizations based on total protein do not reflect local concentrations of CYP27A1 in the neural retina and RPE. The neural retina is a multilayered and multicellular organ with uneven expression of CYP27A1 as assessed by immunohistochemistry (15), whereas the RPE represents one layer of the same cell type. Therefore, concentrations of CYP27A1 in some retinal cells could be comparable to those in the RPE.

DISCUSSION

This study was undertaken to further elucidate cholesterol metabolism in the retina and the role of CYP27A1 in this process. Previously we measured retinal and the RPE content of cholesterol and sterol metabolites generated enzymatically (36). In the present work, we focused on 7KCh, the nonenzymatic product of cholesterol oxidation, and investigated its possible elimination by CYP27A1. By using in vitro assays, we demonstrated for the first time that purified recombinant CYP27A1 binds and metabolizes 7KCh and oxidizes this sterol ~4-fold more efficiently than cholesterol, despite a similar affinity for 7KCh and cholesterol. These data served as the biochemical basis for the search of the C27-hydroxylated metabolites of 7KCh in the retina.

From previous studies by others (8, 9) we knew that 7KCh is present in the retina but its hydroxylated derivatives were not detected by HPLC-MS with atmospheric pressure chemical ionization mode. We also knew that 7KCh is one of the most difficult oxysterols to measure because even minor auto-oxidation of highly abundant cholesterol during sample isolation and workup will lead to falsely high levels of 7KCh and overestimation of its content by as much as a 1,000-fold (35). We were also aware that to accurately quantify 7KCh, as well as any other sterol, its deuterated analog should be added to a biological sample prior to the beginning of any manipulations. Therefore, to assay bovine neural retina and RPE for 7KCh and its C27-oxygenated metabolites, we employed a highly sensitive and accurate GC-MS methodology with SIM detection, used deuterated 7KCh as internal standard, and maintained anaerobic conditions during sample processing.

The measured levels of free 7KCh were in a low picomolar range; they were 1.6-fold higher in the RPE (41 pmol/mg protein) than in the retina (25 pmol/mg of protein) as assessed by the measurements in one preparation. Similar to cholesterol and oxysterols formed enzymatically (36), saponification did not significantly increase the 7KCh content either in the neural retina or RPE, indicating that sulfonation or other types of esterification are unlikely to be the major mechanisms by which retinal cells eliminate or reduce the toxicity of this metabolite. These data are consistent with undetectable retinal levels of mRNA for sulfotransferase 2B1b (4), one of the enzymes that could sulfonate 7KCh (37).

A notable difference between oxysterols generated enzymatically (36) and the nonenzymatically formed 7KCh was a significant interpreparation variability in the levels of the latter. Of the four preparations tested, a 40 picomolar/mg protein concentration of 7KCh was detected only in one preparation of the RPE, whereas the other three preparations contained similar and much lower levels of 7KCh (~8 pmol/mg protein). A 5-fold variation in the content of 7KCh in the RPE could be due to differences in animal housing, feeding, demographics, and duration of

TABLE 2. Quantification of CYP27A1 in human RPE

CYP27A1 peptide	Donor (pmol/mg tissue protein)[a]			
	#12	#13	#17	#20
RPE				
LYPVVPTNSR	1.45 ± 0.12	2.06 ± 0.12	1.11 ± 0.33	1.61 ± 0.23
VVLAPETGELK	1.30 ± 0.16	1.90 ± 0.23	1.15 ± 0.11	1.39 ± 0.10
EIEVDGFLFPK	1.65 ± 0.32	2.08 ± 0.20	1.26 ± 0.12	1.72 ± 0.05
Consensus	1.46 ± 0.24	2.01 ± 0.18	1.17 ± 0.20	1.57 ± 0.19
Neural retina[b]				
Consensus	0.46 ± 0.04	0.51 ± 0.05	0.57 ± 0.05	0.53 ± 0.06

[a]The concentration was calculated for three experimental replicates by monitoring three transitions per individual peptide and presented as mean ± SD. For the consensus, the data for three peptides from CYP27A1 were combined and presented as mean ± SD. The monitored transitions are the same as in Ref. 24.
[b]Taken from Ref. 24.

exposure to sunlight. Studies of the photodamaged rat retinas demonstrated that the levels of 7KCh are increased 6-fold when animals are exposed to intense, constant light (9). The first preparation of the neural retina and RPE was the only one obtained in late spring, whereas the other three preparations were isolated throughout autumn. Despite interpreparation variability, a range of the 7KCh concentrations in our study was still significantly lower than that reported in monkey and rat tissues: 0.21 pmol/nmol of free cholesterol in bovine neural retina versus 1-1.6 pmol/nmol of free cholesterol in untreated monkey and rat retinas; and 0.07-0.36 pmol/nmol of free cholesterol in bovine RPE versus 5-8 pmol/nmol of free cholesterol in monkey RPE-choriocapillaris (8, 9). These differences could represent interspecies variations and be pertinent to the way the quantifications were carried out. In our study, sterol concentrations were determined by plotting the ratio of the ion peak areas (endogenous sterol/deuterated internal standard) against the calibration generated separately for each sterol of interest. In sterol quantifications in monkeys and rats, the concentrations were derived from the peak areas specific to cholesterol and 7KCh after normalization to the peak area of the internal standard β-sitosterol (8, 9). In any case, the range of the 7KCh concentrations in bovine neural retina and RPE (0.07-0.36 pmol/nmol cholesterol) was more comparable to the 7KCh levels in hamster brain ($\sim$0.05 pmol/nmol cholesterol) (38) with higher concentrations in the neural retina possibly reflecting its unique oxidative environment (reviewed in Ref. 4).

Increased levels of 7KCh in the first preparation of bovine RPE enabled the detection of its metabolites, 7KCh-27OH and 7KCh-27COOH, whose identification was based on the coelution of four fragment ions specific for 7KCh-27OH and 7KCh-27COOH at the retention times of the authentic standards. The sites of oxygenation in 7KCh as well as expression in the RPE strongly suggest that 7KCh-27OH and 7KCh-27COOH are the enzymatic products of CYP27A1, consistent with our in vitro studies using purified recombinant enzyme. Furthermore, it is conceivable that 7KCh could be formed in the mitochondrion because the mitochondrial respiratory chain is known to produce reactive oxygen species, which in turn can oxidize cholesterol to yield 7KCh and other products (39, 40). Recent studies also suggest that in the retina cholesterol oxidation could involve ferritin, which colocalizes with 7KCh (9). Ferritin was shown to release bound iron upon light exposure (41) and induce lipid peroxidation in photoreceptor outer segments (42). This mechanism is supported by identification of a new form of ferritin, mitochondrial ferritin, which localizes in the mitochondrial matrix (43).

The steady-state levels of 7KCh-27OH in bovine RPE were $\sim$1/40 of those of 7KCh, and the metabolite to substrate ratio would presumably have been even higher if we could have quantified 7KCh-27COOH. But even when assessed based on 7KCh-27OH, this ratio is more than two orders of magnitude higher than the ratio of the other CYP27A1 metabolite and substrate pair, 27COOH and cholesterol ($\sim$1/14,000) (38). Such high 7KCh-27OH/7KCh ratio

compared with the 27COOH/cholesterol ratio may reflect either more efficient metabolism of 7KCh relative to cholesterol or less efficient elimination of 7KCh-27OH relative to 27COOH. The former would be in agreement with the results of our in vitro studies evaluating cholesterol and 7KCh as the substrates for CYP27A1, as well with prior investigations by others showing cytotoxic, pro-inflammatory, and apoptotic effects of 7KCh on the RPE-derived cells (4, 15, 44). 27-Hydroxylation seems to reduce toxicity of 7KCh as demonstrated by survival of the RPE cells treated with 7KCh-27OH at concentrations and time in which 7KCh essentially killed the entire culture (15). Thus, high 7KCh-27OH/7KCh ratio in a cell would be consistent with attenuated toxicity of 7KCh-27OH relative to 7KCh. Indeed, if a metabolite is as toxic as the parent compound, it will not be accumulated at comparable levels in a cell.

The ability of the RPE to metabolize 7KCh was also confirmed in the incubations with the homogenates from the preparations where the 7KCh content was low ($\sim$8 pmol/mg protein) and its metabolites could not be detected by GC-MS. 7KCh-27OH was formed only when the homogenates were supplemented with the mitochondrial P450 redox system. In these experiments, $\sim$1/5 of 7KCh was converted to 7KCh-27OH, but only $\sim$1/200 of cholesterol was converted to 27OH. More efficient metabolism of 7KCh relative to cholesterol suggested that CYP27A1 should be seriously considered as a contributor to 7KCh elimination from the RPE. Yet studies of other possible elimination pathways are required to assess quantitative significance of 27-hydroxylation in the overall metabolism of 7KCh in the RPE. Also, it is important to identify the carriers of 7KCh-derived oxysterols inside and outside the cell. Oxysterol-binding protein was found to interact with 7KCh and 27OH (45, 46), and oxysterol-binding protein-related protein 2 was found to bind 7KCh (47). 27OH and 27COOH were shown to spontaneously diffuse across plasma membranes and become associated outside the cell either with HDL (27OH) or albumin (27COOH) (48, 49). Conceivably, upon exit from the mitochondrion, 7KCh-27OH could interact with one of the oxysterol transport proteins and be delivered to the plasma membrane, which it quickly traverses, followed by complex formation with either HDL or albumin. This mechanism would be concordant with the finding that the neural retina and RPE express many proteins necessary for HDL lipid transport, for example, apolipoprotein A1 (50), the major component of HDL. Immunohistochemistry localization on monkey retina found apolipoprotein A1 in Bruch's membrane, which represents the interface between the RPE and choroid, as well as on the apical side of the RPE (this side faces the interphotoreceptor matrix and neural retina) and in the interphotoreceptor matrix surrounding the photoreceptor outer segments (50). Thus, 7KCh metabolites can be accepted by HDL on either side of the RPE. Consequently, they can diffuse from the RPE through either apical or basal sides. Yet passive diffusion usually requires a concentration gradient between the donor cell membrane and the extracellular acceptor. Because of the intensity of the choroidal blood flow, the HDL-7KCh me-

tabolite complex will be removed more quickly from the basal side of the RPE than from the apical. Therefore, we hypothesize that the majority of 7KCh metabolites will diffuse through the basal side of the RPE. With respect to physiological relevance, if CYP27A1 is indeed important for elimination of toxic 7KCh from the RPE, CYP27A1 deficiency should lead to accumulation of 7KCh and may affect normal retinal function. Experiments are underway in this laboratory to investigate whether accumulation of 7KCh underlies the formation of retinal pathologies observed in CYP27A1-difficient mice.⬛⬛

REFERENCES

1. Smith, L. L. 1996. Review of progress in sterol oxidations: 1987-1995. *Lipids*. **31:** 453–487.
2. Brown, A. J., and W. Jessup. 1999. Oxysterols and atherosclerosis. *Atherosclerosis*. **142:** 1–28.
3. Jessup, W., and A. J. Brown. 2005. Novel routes for metabolism of 7-ketocholesterol. *Rejuvenation Res*. **8:** 9–12.
4. Rodriguez, I. R., and I. M. Larrayoz. 2010. Cholesterol oxidation in the retina: Implications of 7-ketocholesterol formation in chronic inflammation and age-related macular degeneration. *J. Lipid Res*. **51:** 2847–2862.
5. Hulten, L. M., H. Lindmark, U. Diczfalusy, I. Bjorkhem, M. Ottosson, Y. Liu, G. Bondjers, and O. Wiklund. 1996. Oxysterols present in atherosclerotic tissue decrease the expression of lipoprotein lipase messenger RNA in human monocyte-derived macrophages. *J. Clin. Invest*. **97:** 461–468.
6. Girao, H., M. C. Mota, J. Ramalho, and P. Pereira. 1998. Cholesterol oxides accumulate in human cataracts. *Exp. Eye Res*. **66:** 645–652.
7. Girao, H., F. Shang, and P. Pereira. 2003. 7-ketocholesterol stimulates differentiation of lens epithelial cells. *Mol. Vis*. **9:** 497–501.
8. Moreira, E. F., I. M. Larrayoz, J. W. Lee, and I. R. Rodriguez. 2009. 7-Ketocholesterol is present in lipid deposits in the primate retina: potential implication in the induction of VEGF and CNV formation. *Invest. Ophthalmol. Vis. Sci*. **50:** 523–532.
9. Rodriguez, I. R., and S. J. Fliesler. 2009. Photodamage generates 7-keto- and 7-hydroxycholesterol in the rat retina via a free radical-mediated mechanism. *Photochem. Photobiol*. **85:** 1116–1125.
10. Klein, R., T. Peto, A. Bird, and M. R. Vannewkirk. 2004. The epidemiology of age-related macular degeneration. *Am. J. Ophthalmol*. **137:** 486–495.
11. Jager, R. D., W. F. Mieler, and J. W. Miller. 2008. Age-related macular degeneration. *N. Engl. J. Med*. **358:** 2606–2617.
12. Wikvall, K. 1984. Hydroxylations in biosynthesis of bile acids. Isolation of a cytochrome P-450 from rabbit liver mitochondria catalyzing 26-hydroxylation of C27-steroids. *J. Biol. Chem*. **259:** 3800–3804.
13. Okuda, K., O. Masumoto, and Y. Ohyama. 1988. Purification and characterization of 5 beta-cholestane-3 alpha,7 alpha,12 alpha-triol 27-hydroxylase from female rat liver mitochondria. *J. Biol. Chem*. **263:** 18138–18142.
14. Masumoto, O., Y. Ohyama, and K. Okuda. 1988. Purification and characterization of vitamin D 25-hydroxylase from rat liver mitochondria. *J. Biol. Chem*. **263:** 14256–14260.
15. Lee, J. W., H. Fuda, N. B. Javitt, C. A. Strott, and I. R. Rodriguez. 2006. Expression and localization of sterol 27-hydroxylase (CYP27A1) in monkey retina. *Exp. Eye Res*. **83:** 465–469.
16. Brown, A. J., G. F. Watts, J. R. Burnett, R. T. Dean, and W. Jessup. 2000. Sterol 27-hydroxylase acts on 7-ketocholesterol in human atherosclerotic lesions and macrophages in culture. *J. Biol. Chem*. **275:** 27627–27633.
17. Lyons, M. A., and A. J. Brown. 2001. Metabolism of an oxysterol, 7-ketocholesterol, by sterol 27-hydroxylase in HepG2 cells. *Lipids*. **36:** 701–711.
18. Pikuleva, I. A., I. Bjorkhem, and M. R. Waterman. 1997. Expression, purification, and enzymatic properties of recombinant human cytochrome P450c27 (CYP27). *Arch. Biochem. Biophys*. **343:** 123–130.
19. Sagara, Y., T. Hara, Y. Ariyasu, F. Ando, N. Tokunaga, and T. Horiuchi. 1992. Direct expression in *Escherichia coli* and characterization of bovine adrenodoxins with modified amino-terminal regions. *FEBS Lett*. **300:** 208–212.
20. Sagara, Y., A. Wada, Y. Takata, M. R. Waterman, K. Sekimizu, and T. Horiuchi. 1993. Direct expression of adrenodoxin reductase in *Escherichia coli* and the functional characterization. *Biol. Pharm. Bull*. **16:** 627–630.
21. Hanna, I. H., J. F. Teiber, K. L. Kokones, and P. F. Hollenberg. 1998. Role of the alanine at position 363 of cytochrome P450 2B2 in influencing the NADPH- and hydroperoxide-supported activities. *Arch. Biochem. Biophys*. **350:** 324–332.
22. Heller, J., and P. Jones. 1980. Purification of bovine retinal pigment epithelial cells by dissociation in calcium free buffers and centrifugation in Ficoll density gradients followed by "recovery" in tissue culture. *Exp. Eye Res*. **30:** 481–487.
23. Berman, E. R., H. Schwell, and L. Feeney. 1974. The retinal pigment epithelium. Chemical composition and structure. *Invest. Ophthalmol*. **13:** 675–687.
24. Liao, W. L., G. Y. Heo, N. G. Dodder, R. E. Reem, N. Mast, S. Huang, P. L. Dipatre, I. V. Turko, and I. A. Pikuleva. 2011. Quantification of cholesterol-metabolizing P450s CYP27A1 and CYP46A1 in neural tissues reveals a lack of enzyme-product correlations in human retina but not human brain. *J. Proteome Res*. **10:** 241–248.
25. Folch, J., M. Lees, and G. H. Sloane Stanley. 1957. A simple method for the isolation and purification of total lipides from animal tissues. *J. Biol. Chem*. **226:** 497–509.
26. Juaneda, P., and G. Rocquelin. 1985. Rapid and convenient separation of phospholipids and non phosphorus lipids from rat heart using silica cartridges. *Lipids*. **20:** 40–41.
27. Stewart, J. C. 1980. Colorimetric determination of phospholipids with ammonium ferrothiocyanate. *Anal. Biochem*. **104:** 10–14.
28. Mast, N., D. Murtazina, H. Liu, S. E. Graham, I. Bjorkhem, J. R. Halpert, J. Peterson, and I. A. Pikuleva. 2006. Distinct binding of cholesterol and 5beta-cholestane-3alpha,7alpha,12alpha-triol to cytochrome P450 27A1: evidence from modeling and site-directed mutagenesis studies. *Biochemistry*. **45:** 4396–4404.
29. Copeland, R. A., editor. 2000. Protein-ligand binding equilibria. *In* Enzymes: A Practical Introduction to Structure, Mechanism, and Data Analysis. 2nd edition. Wiley-VCH, New York. 76–108.
30. Griffiths, W. J., M. Hornshaw, G. Woffendin, S. F. Baker, A. Lockhart, S. Heidelberger, M. Gustafsson, J. Sjovall, and Y. Wang. 2008. Discovering oxysterols in plasma: a window on the metabolome. *J. Proteome Res*. **7:** 3602–3612.
31. Brown, A. J., S. L. Leong, R. T. Dean, and W. Jessup. 1997. 7-Hydroperoxycholesterol and its products in oxidized low density lipoprotein and human atherosclerotic plaque. *J. Lipid Res*. **38:** 1730–1745.
32. Pikuleva, I. A., A. Babiker, M. R. Waterman, and I. Bjorkhem. 1998. Activities of recombinant human cytochrome P450c27 (CYP27) which produce intermediates of alternative bile acid biosynthetic pathways. *J. Biol. Chem*. **273:** 18153–18160.
33. Cali, J. J., and D. W. Russell. 1991. Characterization of human sterol 27-hydroxylase. A mitochondrial cytochrome P-450 that catalyzes multiple oxidation reactions in bile acid biosynthesis. *J. Biol. Chem*. **266:** 7774–7778.
34. Daum, G. 1985. Lipids of mitochondria. *Biochim. Biophys. Acta*. **822:** 1–42.
35. Leoni, V., D. Lutjohann, and T. Masterman. 2005. Levels of 7-oxocholesterol in cerebrospinal fluid are more than one thousand times lower than reported in multiple sclerosis. *J. Lipid Res*. **46:** 191–195.
36. Mast, N., R. Reem, I. Bederman, S. Huang, P. L. DiPatre, I. Bjorkhem, and I. A. Pikuleva. 2011. Cholestenoic acid is an important elimination product of cholesterol in the retina: comparison of retinal cholesterol metabolism to that in the brain. *Invest. Ophthalmol. Vis. Sci*. **52:** 594–603.
37. Fuda, H., N. B. Javitt, K. Mitamura, S. Ikegawa, and C. A. Strott. 2007. Oxysterols are substrates for cholesterol sulfotransferase. *J. Lipid Res*. **48:** 1343–1352.

38. Mast, N., M. Shafaati, W. Zaman, W. Zheng, D. Prusak, T. Wood, G. A. Ansari, A. Lovgren-Sandblom, M. Olin, I. Bjorkhem, et al. 2010. Marked variability in hepatic expression of cytochromes CYP7A1 and CYP27A1 as compared to cerebral CYP46A1. Lessons from a dietary study with omega 3 fatty acids in hamsters. *Biochim. Biophys. Acta.* **1801:** 674–681.

39. Girotti, A. W., and W. Korytowski. 2000. Cholesterol as a singlet oxygen detector in biological systems. *Methods Enzymol.* **319:** 85–100.

40. Girotti, A. W., and T. Kriska. 2004. Role of lipid hydroperoxides in photo-oxidative stress signaling. *Antioxid. Redox Signal.* **6:** 301–310.

41. Ohishi, K., X. M. Zhang, S. Moriwaki, T. Hiramitsu, and S. Matsugo. 2005. Iron release analyses from ferritin by visible light irradiation. *Free Radic. Res.* **39:** 875–882.

42. Ohishi, K., X. M. Zhang, S. Moriwaki, T. Hiramitsu, and S. Matsugo. 2006. In the presence of ferritin, visible light induces lipid peroxidation of the porcine photoreceptor outer segment. *Free Radic. Res.* **40:** 799–807.

43. Levi, S., B. Corsi, M. Bosisio, R. Invernizzi, A. Volz, D. Sanford, P. Arosio, and J. Drysdale. 2001. A human mitochondrial ferritin encoded by an intronless gene. *J. Biol. Chem.* **276:** 24437–24440.

44. Larrayoz, I. M., J. D. Huang, J. W. Lee, I. Pascual, and I. R. Rodriguez. 2010. 7-ketocholesterol-induced inflammation: involvement of multiple kinase signaling pathways via NFkappaB but independently of reactive oxygen species formation. *Invest. Ophthalmol. Vis. Sci.* **51:** 4942–4955.

45. Taylor, F. R., S. E. Saucier, E. P. Shown, E. J. Parish, and A. A. Kandutsch. 1984. Correlation between oxysterol binding to a cytosolic binding protein and potency in the repression of hydroxymethylglutaryl coenzyme A reductase. *J. Biol. Chem.* **259:** 12382–12387.

46. Dawson, P. A., D. R. Van der Westhuyzen, J. L. Goldstein, and M. S. Brown. 1989. Purification of oxysterol binding protein from hamster liver cytosol. *J. Biol. Chem.* **264:** 9046–9052.

47. Hynynen, R., M. Suchanek, J. Spandl, N. Back, C. Thiele, and V. M. Olkkonen. 2009. OSBP-related protein 2 is a sterol receptor on lipid droplets that regulates the metabolism of neutral lipids. *J. Lipid Res.* **50:** 1305–1315.

48. Meaney, S., K. Bodin, U. Diczfalusy, and I. Bjorkhem. 2002. On the rate of translocation in vitro and kinetics in vivo of the major oxysterols in human circulation: critical importance of the position of the oxygen function. *J. Lipid Res.* **43:** 2130–2135.

49. Babiker, A., O. Andersson, E. Lund, R. J. Xiu, S. Deeb, A. Reshef, E. Leitersdorf, U. Diczfalusy, and I. Bjorkhem. 1997. Elimination of cholesterol in macrophages and endothelial cells by the sterol 27-hydroxylase mechanism. Comparison with high density lipoprotein-mediated reverse cholesterol transport. *J. Biol. Chem.* **272:** 26253–26261.

50. Tserentsoodol, N., N. V. Gordiyenko, I. Pascual, J. W. Lee, S. J. Fliesler, and I. R. Rodriguez. 2006. Intraretinal lipid transport is dependent on high density lipoprotein-like particles and class B scavenger receptors. *Mol. Vis.* **12:** 1319–1333.